AFRL-RY-WP-TR-2013-0174

RADIATION CHARACTERISTICS OF ANTENNAS EMBEDDED IN A LAYER WITH TWO-TEMPERATURE ELECTRON POPULATION

Saba Mudaliar

Antennas and Electromagnetics Technology Branch
Multispectral Sensing and Detection Division

OCTOBER 2013
Interim Report

AIR FORCE RESEARCH LABORATORY
SENSORS DIRECTORATE
WRIGHT-PATTERSON AIR FORCE BASE, OH 45433-7320
AIR FORCE MATERIEL COMMAND
UNITED STATES AIR FORCE

NOTICE AND SIGNATURE PAGE

Using Government drawings, specifications, or other data included in this document for any purpose other than Government procurement does not in any way obligate the U.S. Government. The fact that the Government formulated or supplied the drawings, specifications, or other data does not license the holder or any other person or corporation; or convey any rights or permission to manufacture, use, or sell any patented invention that may relate to them.

This report was cleared for public release by the USAF 88th Air Base Wing (88 ABW) Public Affairs Office and is available to the general public, including foreign nationals. Copies may be obtained from the Defense Technical Information Center (DTIC) (http://www.dtic.mil).

AFRL-RY-WP-TR-2013-0174 HAS BEEN REVIEWED AND IS APPROVED FOR PUBLICATION IN ACCORDANCE WITH ASSIGNED DISTRIBUTION STATEMENT.

//SIGNED//

SABA MUDALIAR, Program Manager
Antennas and Electromagnetics Technology Branch
Multispectral Sensing and Detection Division

//SIGNED//

TONY KIM, Chief
Antennas and Electromagnetics Technology Branch
Multispectral Sensing and Detection Division

//SIGNED//

TRACY W. JOHNSTON, Chief
Multispectral Sensing and Detection Division
Sensors Directorate

This report is published in the interest of scientific and technical information exchange, and its publication does not constitute the Government's approval or disapproval of its ideas or findings.

*Disseminated copies will show "//signature//" stamped or typed above the signature blocks.

REPORT DOCUMENTATION PAGE

Form Approved
OMB No. 0704-0188

1. REPORT DATE *(DD-MM-YY)*	2. REPORT TYPE	3. DATES COVERED *(From - To)*
October 2013	Interim	1 October 2011 – 30 September 2013

4. TITLE AND SUBTITLE
RADIATION CHARACTERISTICS OF ANTENNAS EMBEDDED IN A LAYER WITH TWO-TEMPERATURE ELECTRON POPULATION

5a. CONTRACT NUMBER
In-house

5b. GRANT NUMBER

5c. PROGRAM ELEMENT NUMBER
61102F

6. AUTHOR(S)
Saba Mudaliar

5d. PROJECT NUMBER
3002

5e. TASK NUMBER
HE

5f. WORK UNIT NUMBER
Y0NH

7. PERFORMING ORGANIZATION NAME(S) AND ADDRESS(ES)
Antennas and Electromagnetics Technology Branch
Multispectral Sensing and Detection Division
Air Force Research Laboratory, Sensors Directorate
Wright-Patterson Air Force Base, OH 45433-7320
Air Force Materiel Command, United States Air Force

8. PERFORMING ORGANIZATION REPORT NUMBER
AFRL-RY-WP-TR-2013-0174

9. SPONSORING/MONITORING AGENCY NAME(S) AND ADDRESS(ES)
Air Force Research Laboratory
Sensors Directorate
Wright-Patterson Air Force Base, OH 45433-7320
Air Force Materiel Command
United States Air Force

Air Force Office of Scientific Research
Public Affairs (AFOSR)
875 North Randolph St. Suite 325, Rm3112
Arlington, VA 22203-1768

10. SPONSORING/MONITORING AGENCY ACRONYM(S)
AFRL/RYMH

11. SPONSORING/MONITORING AGENCY REPORT NUMBER(S)
AFRL-RY-WP-TR-2013-0174

12. DISTRIBUTION/AVAILABILITY STATEMENT
Approved for public release; distribution unlimited.

13. SUPPLEMENTARY NOTES
PAO Case Number 88ABW-2013-4275, Clearance Date 7 October 2013. Report contains color.

14. ABSTRACT
It is well-known that low frequency electromagnetic (EM) signals are heavily attenuated in a medium with dense electron population. If we create in this medium a small population of relatively hot electrons the composite medium then supports low-frequency electrostatic oscillations known as electron acoustic waves (EAW). The dispersion relation of this composite medium shows that it supports EAW in the frequency band where EM signals are cut off. Our primary interest in this report is to study the radiation characteristics of a source current distribution embedded in a half-space of our composite medium. To enable this, we derive the Green's functions for our problem and hence study the radiation characteristics of antennas. When the source signal frequency is below the plasma frequency, only EAW exist in the composite medium, while only EM waves can exist in the free space above. We find that the far-zone radiation fields of any current distribution consist only of θ-polarized waves. We find that in both cases the radiation patterns are skewed towards the horizon. In particular, we find that the radiation pattern of a horizontal dipole has two lobes as opposed to one in the underdense case.

15. SUBJECT TERMS
dispersion relation, electron acoustic waves, overdense plasma, Hertzian dipole, radiation characteristics

16. SECURITY CLASSIFICATION OF:			17. LIMITATION OF ABSTRACT:	18. NUMBER OF PAGES	19a. NAME OF RESPONSIBLE PERSON (Monitor)
a. REPORT	b. ABSTRACT	c. THIS PAGE			Saba Mudaliar
Unclassified	Unclassified	Unclassified	SAR	34	19b. TELEPHONE NUMBER *(Include Area Code)* N/A

1. Summary

It is well-known that low frequency electromagnetic (EM) signals are heavily attenuated in a medium with dense electron population. All signals below the plasma frequency of the medium get cut off. If we create in this medium a small population of relatively hot electrons the composite medium then supports low-frequency electrostatic oscillations known as electron acoustic waves (EAW) [e.g., Gary and Tokar, *Phys. Fluids*, vol. 28, p 2439]. The dispersion relation of this composite medium shows that it supports EAW in the frequency band where EM signals are cut off. Thus it is possible, in principle, to employ EAW to transmit signals across an overdense plasma medium. Our primary interest in this report is to study the radiation characteristics of a source current distribution embedded in a half-space of our composite medium. To enable this, we derive the Green's functions for our problem and hence study the radiation characteristics of antennas. When the source signal frequency is below the plasma frequency, only EAW exist in the composite medium, while only EM waves can exist in the free space above. We find that the far-zone radiation fields of any current distribution consist only of θ-polarized waves. Explicit expressions for the radiated fields are obtained for horizontally- and vertically-polarized Hertzian dipoles embedded in our composite medium. We hence find that in both cases the radiation patterns are skewed towards the horizon. In particular, we find that the radiation pattern of a horizontal dipole has two lobes as opposed to one in the underdense case.

2. Introduction

When a space vehicle reenters the atmosphere it encounters a bow shock. The kinetic energy of the vehicle is translated into high heat and pressure in the shock layer. This initiates a variety of thermo-chemical processes [1], [2] and a dense plasma sheath surrounds the vehicle. It is well-known that sensor performance aboard hypersonic vehicles is degraded to various degrees because of the dense plasma. In our study we have found that there will be periods in the course of the trajectory where the electron density of the plasma sheath is so high that the microwave signals are completely cut off. This is the famous ``communication blackout'' encountered during the Apollo missions in the 1960s. Indeed issues with communication with reentry vehicles were studied even before Apollo missions [3]. Such communication blackout problems are also encountered in many other space exploration missions [4]. Some of early schemes that were proposed are: use of electron beams [5], high frequency laser [6], strong static magnetic fields [5]-[8], and alteration of chemical composition [9]-[13].

Two articles that summarize early ideas are those of Rawhouser [5] and Rybak [14]. More recent ideas put forward are: three-wave scattering process [15], [16], Hall effect drift [17], electrostatic manipulation [17]-[19], and resonant transmission [20], [21]. These schemes exploit the wave phenomenology in the plasma sheath to transmit signals across the sheath. There have also been suggestions on mechanical structures that can avoid the blackout condition. One idea is that of a remote antenna assembly [22] just outside the potential dense plasma region. Also, the choice of shape of the hypersonic vehicle has an important influence on the character of the flow field [23]. Hence it is possible to choose the shape of the vehicle such that blackout situations are minimized. All these schemes have their share of advantages and disadvantages. None have been implemented successfully in any hypersonic vehicles thus far. Indeed there is a long way to go before any of these schemes can be implemented in operational hypersonic vehicles because there remain many theoretical and practical issues to be overcome. Some of the difficulties one faces are: (a) size, weight constraint, (b) engineering issues of implementation, (c) power resources constraint. Furthermore, the proposed concepts have been illustrated only for idealized models; the feasibility and success of such concepts are questionable under non-ideal conditions encountered in practice. Hence the issue of communication blackout is as ``topical'' as it was during Apollo missions [24], [25]. Although there are now other means to communicate (via satellite) the sensor needs for modern hypersonic vehicles are now much greater and more critical. One concept that we are currently investigating is to employ electron acoustic waves (EAW) for carrying low-frequency microwave signals across the overdense plasma sheath [26]. The idea is to create a small population of high temperature electrons into the plasma sheath so that we have a two-temperature electron population. One way to create this composite medium is by injecting hot electrons by an electron gun as it was done during CHARGE-2B experiments [27]-[29]. Although EAW have not been popularly studied in the literature there are a few interesting papers [28], [30] where they play important roles in the context of ionosphere and space experiments. Indeed there are several instances where a two-temperature electron population occurs in nature. Some examples are: earth's bow shock [31], [32], undisturbed solar wind [35], interplanetary shocks [36]. In these contexts the

concept of EAW are sometimes employed to offer theoretical explanation to certain phenomenology.

Note that it is not mandatory to have a two-temperature electron population to excite EAW. One may as well have a single electron population along with a resonant electron beam to excite EAW [37]. Although we have not explored this path in detail we feel that the domain of applicability of our scheme will be much larger than that using single electron population. These remarks are based on the assumption that the electrons have Maxwellian distribution. Furthermore, there are other ways (see for example, [37], [38]), besides that using a resonant electron beam, for creating a plateau near the region of phase velocity of EAW. However, not all such schemes are suitable for use in hypersonic vehicles. Since we have more familiarity and confidence in the beam concept for our application, our study is restricted to this idea.

In this report we show that the two-temperature electron population supports electron acoustic waves [39]-[41] in the frequency domain where the low-frequency electromagnetic waves are cut off. In fact the dispersion relation shows that the propagation characteristics of EM waves and EAW complement each other. Thus it is a promising idea to employ EAW to carry low-frequency microwave signals across an over dense plasma slab. However, there are issues: one of them is the phenomenon of resonant damping. A kinetic approach is taken to understand the damping characteristics of EAW. We also investigate the radiation characteristics of Hertzian dipole antennas embedded in the two-temperature composite medium. In this connection we derive the Green's function for our overdense plasma layer. We hence find that the radiation characteristics of antennas in an overdense two-temperature electron population are quite different from those in free space: (a) only θ-polarized waves are radiated, (b) radiation patter is skewed towards the horizon and (c) the radiation pattern of a horizontal dipole has two lobes as opposed to one in the underdense case.

3.0 Methods, Assumptions, and Procedures

3.1 Electromagnetic Waves

First we study the characteristics of electromagnetic waves (EMW) in our problem. Maxwell's equations are given as

$$\nabla \times \mathbf{H} + \tfrac{i\omega}{c}\mathbf{E} - \tfrac{4\pi}{c}\mathbf{j} = \tfrac{4\pi}{c}\mathbf{J} \tag{1}$$

$$\nabla \times \mathbf{E} = \tfrac{i\omega}{c}\mathbf{H} \tag{2}$$

Here $\mathbf{J}$ is the source current exciting the system; $\mathbf{j}$ is the current distribution due to the plasma sheath given as

$$\mathbf{j} = -en_o\mathbf{v} \tag{3}$$

where e is the electron charge and n_o is the unperturbed electron charge density. The velocity $\mathbf{v}$ of the electrons is governed by the following linearized equation of motion:

$$\partial_t \mathbf{v} + \tfrac{T\nabla n}{mn_o} = -\tfrac{e}{m}\mathbf{E} \tag{4}$$

where T is the electron temperature and m is the electron mass. Note that we have neglected here the electron-neutral collisions[1]. The density and velocity of the electrons are connected by the continuity equation

$$\partial_t n + \nabla \cdot (n_o\mathbf{v}) = 0 \tag{5}$$

On taking the curl of (2) and inserting (1) in it we obtain

$$\nabla \times \nabla \times \mathbf{E} - k^2\mathbf{E} - \tfrac{4\pi i\omega e n_o}{c^2}\mathbf{v} = \tfrac{4\pi i\omega}{c^2}\mathbf{J} \tag{6}$$

where $k = \omega/c$ is the free space wave number. From the equation of motion, we have

$$\mathbf{v} = \tfrac{e}{i\omega m}\mathbf{E} \tag{7}$$

Substituting (7) in (6) we obtain the following equation for the electromagnetic waves

$$\nabla \times \nabla \times \mathbf{E} - k_e^2\mathbf{E} = \tfrac{4\pi i\omega}{c^2}\mathbf{J} \tag{8}$$

where

$$k_e^2 = k^2\left(1 - \tfrac{\omega_p^2}{\omega^2}\right) \tag{9}$$

and ω_p is the plasma frequency given as

$$\omega_p^2 = \tfrac{4\pi e^2 n_o}{m} \tag{10}$$

[1] Collisions will not affect the fundamental character of EMW or the electron acoustic waves. They will only add attenuation to them.

When $\omega > \omega_p$, then k_e^2 is less than k^2 and is positive.This means that the medium will support propagating electromagnetic waves. On the other hand when $\omega < \omega_p$, k_e^2 is negative and the electromagnetic waves here become evanescent [2]. The dispersion relation of the EMW is given as

$$\omega^2 = \omega_p^2 + k_e^2 c^2 \qquad (11)$$

Thus we see that ω_p is the cutoff frequency. All signals with frequency components below ω_p are cut off. Notice that ω_p is proportional $\sqrt{n_o}$, and hence, the cutoff frequency increases with increasing density. The dispersion relation is graphically displayed in Figure 1.

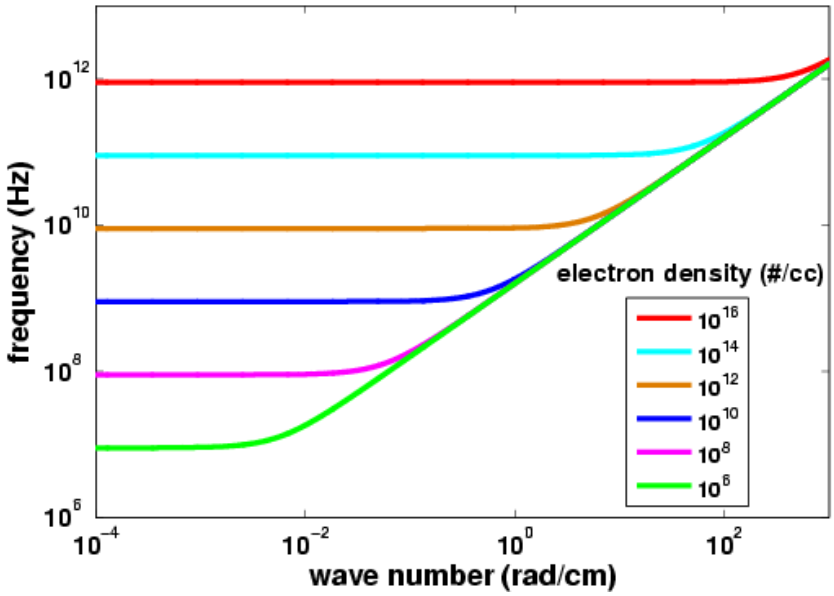

Fig. 1. Dispersion relation of electromagnetic waves for various electron densities

We have plotted frequency versus wave number for various electron densities (cm^{-3}). We have considered electron densities in the range 10^6 to 10^{16}. The range of parameters that describe the hypersonic environment is very large. Several factors such as velocity, altitude, trajectory, shape and size of the vehicle, and heat shield materials have strong influence on the environment. Notice that for $n = 10^{10}$, GPS signals are cut off; at $n = 10^{12}$, communications, telemetry, and radar signals are cut off[3]. Therefore the problem that we may encounter is quite serious. Although several remedies have been suggested, all have their share of limitations and shortcomings. For instance, there are engineering issues, size-weight constraints, and system integration issues. Also, most mitigation ideas have only been proposed and illustrated by assuming simplified ideal conditions. We are currently exploring the idea of employing the electron acoustic waves in a two-temperature electron population. One can inject a small population of hot electrons such that we have a composite medium consisting of cold and hot electrons. We find that such a composite medium can

[2] This situation is called the overdense condition. The other situation when $\omega > \omega_p$ is called the underdense condition.

[3] The interest in this report is the domain when the thickness of the plasma sheath is much larger than the skin depth of the EMW.

support stable electron acoustic waves. We see that the propagation characteristics of EAW in our medium complement those of EMW in the sense that EAW propagate in the frequency band where EMW are cut off. Hence it is a good idea to employ EAW to carry low-frequency EMW across an overdense plasma sheath.

3.2 Electron Acoustic Waves

We employ a hydrodynamic description of the two-temperature electron population problem. The governing equations are the same as in (1), (2), (3), and (5). But now the current due to the charge distribution has two components: one due to hot electrons and the other due to cold electrons. Hence

$$\mathbf{j} = -en_{oc}v_c - en_{oh}v_h \tag{12}$$

where subscripts h and v stand for hot and cold electrons. There are thus two linearized equations of motion (one for hot and one for cold electrons):

$$\partial_t \mathbf{v}_\alpha + \tfrac{T_\alpha \nabla n}{m n_{o\alpha}} = -\tfrac{e}{m}\mathbf{E} \qquad \alpha = \{h, c\} \tag{13}$$

Also, there are two continuity equations given as

$$\partial_t n_\alpha + \nabla \cdot (n_{o\alpha}\mathbf{v}_\alpha) = 0 \tag{14}$$

We apply the divergence and time-derivative operator on the first Maxwell's equation to get

$$\omega^2 \nabla \cdot E + 4\pi e \partial_t \left\{ n_{oc} \nabla \cdot \mathbf{v}_c + n_{oh} \nabla \cdot \mathbf{v}_h \right\} = -4\pi i \omega \nabla \cdot \mathbf{J} \tag{15}$$

We have assumed that the unperturbed charge densities n_{oc} and n_{oh} are constants in our problem. For the case of cold electrons, we assume that T_c is small and neglect the term involving T_c in the equation of motion. Thus

$$\partial_t \mathbf{v}_c \approx -\tfrac{e}{m}\mathbf{E} \tag{16}$$

Further note that EAW are longitudinal and hence irrotational. Hence we express $\mathbf{E}$ as the gradient of the scalar potential ψ. Thus

$$4\pi e n_{oc} \partial_t \nabla \cdot \mathbf{v}_c = -\omega_c^2 \nabla^2 \psi \tag{17}$$

where ω_c is the plasma frequency of the cold electrons. For the hot electrons we use the continuity equation to express $\nabla \cdot \mathbf{v}_h$ and use the following relation obtained from the linearized equation of motion:

$$\tfrac{T_h}{m n_{oh}} \nabla n_h \approx -\tfrac{e}{m}\mathbf{E} \tag{18}$$

Thus

$$4\pi e n_{oh} \partial_t \nabla \cdot \mathbf{v}_h = -\tfrac{\omega^2}{r_h^2}\psi \tag{19}$$

where r_h is the Debye radius of the hot electrons defined as

$$r_h = \tfrac{V_h}{\omega_h} \tag{20}$$

where V_h and ω_h are the thermal speed and plasma frequency of the hot electrons. On substituting (17) and (19) in (15) we obtain the following equation for EAW:

$$\nabla^2\psi + k_a^2\psi = \frac{4\pi i\omega}{\omega_c^2-\omega^2}\nabla\cdot\mathbf{J} \tag{21}$$

with

$$k_a^2 = \frac{1}{r_h^2}\frac{\omega^2}{\omega_c^2-\omega^2} \tag{22}$$

where k_a is the wave number of EAW in our composite medium. Thus the dispersion relation for EAW is given as

$$\omega^2 = \frac{\omega_c^2}{1+k^{-2}r_h^{-2}} \tag{23}$$

Notice that in contrast to EMW the plasma frequency is now the upper cutoff frequency. In other words, the medium supports EAW only with frequencies less than the plasma frequency of the cold electron population. The dispersion relation of EAW is graphically displayed in Figure 2. We have chosen the hot electron density to be 5% of the total electron population and its temperature to be 20 eV. Since the cold electron temperature is taken as 0.2 eV we have a temperature contrast ratio of 100.

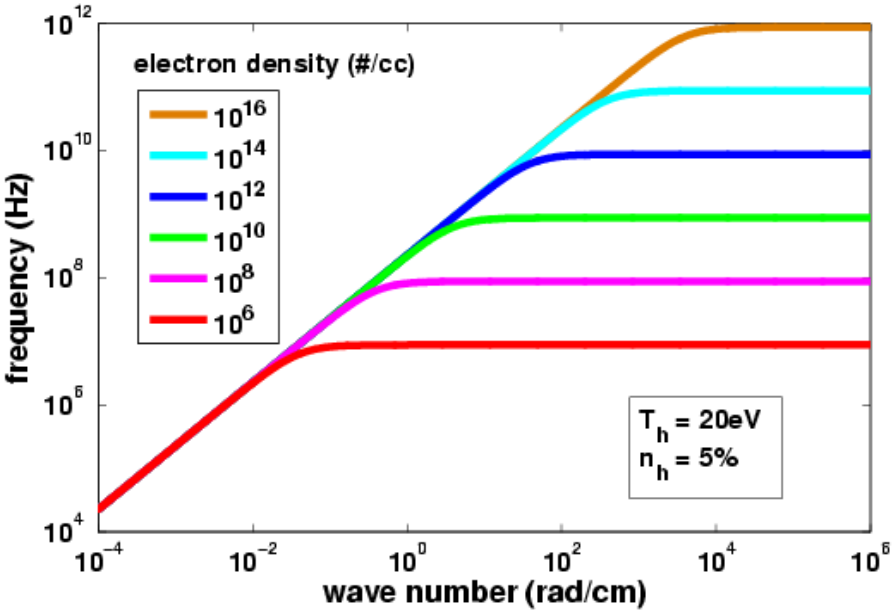

Figure 2. Dispersion relation of electron acoustic waves for various total electron densities

It is instructive to compare Figures 1 and 2. Both graphs have the same set of electron densities. Notice that for EMW the plasma frequency is the lower bound of its pass band. In contrast, for EAW the plasma frequency is the upper bound of its pass band. In that sense they are exact complements. However, there are differences in the manner in which they approach cutoff. In the case of EMW $\omega/k \to c$ for $\omega \gg \omega_{pe}$. In the case of EAW, $\omega/k \to V_h\sqrt{n_e/n_h}$ for $\omega \ll \omega_{pe}$.

Two basic quantities characterizing waves are phase velocity (v_p) and group velocity (v_g), which are defined as

$$v_p = \frac{\omega}{k} \qquad v_g = \frac{\partial \omega}{\partial k} \tag{24}$$

For the case of EMW,

$$v_p = \frac{c}{\nu} \qquad \nu = \left(1 - \frac{\omega_c^2}{\omega^2}\right)^{\frac{1}{2}} \qquad \omega > \omega_c \tag{25}$$

Since $\nu < 1$, the phase velocity of the EMW is larger than c However the group velocity is νc and hence is less than c.

For the case of EAW,

$$v_p = \frac{\omega_c}{k}\sqrt{\delta} \ , \qquad v_g = v_p \nu \delta \qquad \delta = \frac{k^2 r_h^2}{1+k^2 r_h^2} \tag{26}$$

EMW may be considered as constant velocity waves (as is evident for large k) while EAW are constant frequency waves. For large wave numbers the phase velocity of EMW approaches the constant value c. In contrast the phase velocity of EAW decreases with increase in k. Thus the group velocity of EAW vanishes for large k. However, we will see that EAW are weakly damped only for $kr_h \ll 1$ and, hence, we will operate in the domain where the group velocity is nonzero so that we can carry low-frequency signals across the overdense plasma sheath using EAW.

3.3 Green's Function of Electron Acoustic Waves

In order to understand the radiation characteristics of EAW we now derive their Green's function. The governing equation is (21). The conservation equation for source current there is given as

$$\nabla \cdot \mathbf{J} + \partial_t q = 0 \tag{27}$$

where q is the charge density of the source. Inserting this relation in (21), we obtain

$$\nabla^2 \psi + k_a^2 \psi = -4\pi q k_a^2 r_h^2 \tag{28}$$

Employing the Fourier transform we obtain the following solution:

$$\psi(\mathbf{k}, \omega) = \frac{k_a^2 r_h^2}{k^2 - k_a^2} 4\pi q \tag{29}$$

Thus

$$\psi(\mathbf{r}, \omega) = \frac{1}{(2\pi)^3} \int \frac{k_a^2 r_h^2}{k^2 - k_a^2} 4\pi q e^{i\mathbf{k}\cdot\mathbf{r}} d\mathbf{k} \tag{30}$$

To evaluate the integral we introduce polar coordinates k, θ, ϕ as $k_x = k \sin\theta \cos\phi$, $k_y = k \sin\theta \sin\phi$, $k_z = k \cos\theta$ and assume, without loss of generality, that $\mathbf{r} = R\,\hat{z}$. Thus we have

$$\begin{aligned} \psi(\mathbf{r}, \omega) &= \frac{q k_a^2 r_h^2}{\pi} \int_0^\infty \frac{k^2}{k^2 - k_a^2} \int_0^\pi e^{ikR\cos\theta} \sin\theta \, d\theta \, dk \\ &= \frac{q k_a^2 r_h^2}{\pi} \int_{-\infty}^\infty \frac{k^2 e^{ikR}}{k^2 - k_a^2} dk \end{aligned} \tag{31}$$

Since EAW undergo resonant damping (as will be seen in the next section) k_a is complex. The integrand thus has two poles, at $k = \pm k_a$ as shown in Figure 3. Noting that $e^{ikR} = e^{ik'R} e^{-k''R}$ (k' and k'' are the real and imaginary parts of k), we choose the contour of integration along the semi-circle in the upper half plane as shown in the figure. Since the integrand vanishes along the semi-circular path the integral in (31) becomes

$$\oint_C \frac{k^2 e^{ikR}}{k^2 - k_a^2} dk = \pi i e^{ik_a R} \tag{32}$$

where C denotes the contour shown in Figure 3. Substituting this in (31), we obtain

$$\psi(\mathbf{r}, \omega) = \frac{2 q k_a^2 r_h^2}{R} e^{ik_a R} \tag{33}$$

From this we obtain the space-time potential of EAW as

$$\psi(\mathbf{r}, t) = \frac{1}{2\pi} \int_{-\infty}^{-\infty} \psi(r, \omega) e^{-i\omega t} d\omega \tag{34}$$

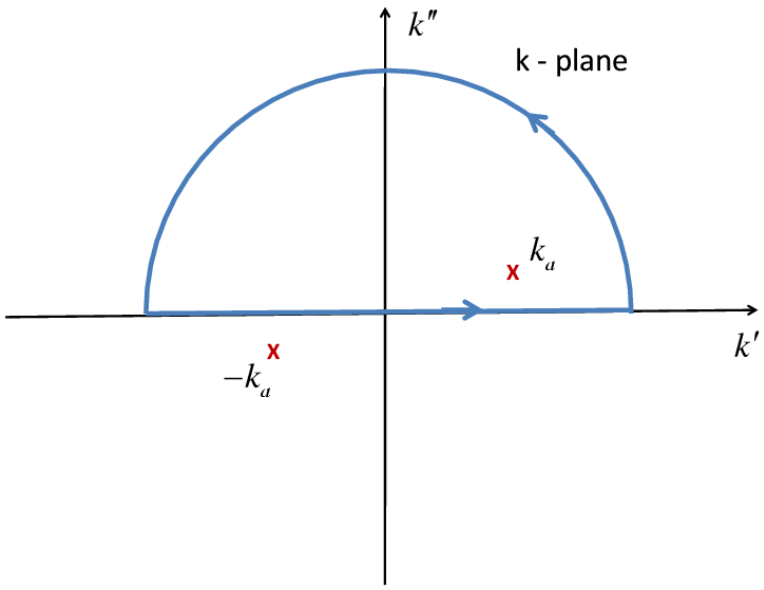

Figure 3. Integration Contour for EAW in the k -plane.

The propagation constant of EAW is given as

$$k_a = \frac{\omega}{c_a}, \quad c_a = r_h\sqrt{\omega_c^2 - \omega^2} \tag{35}$$

where c_a is the phase velocity of EAW which, as shown above, varies with frequency. This dispersive character makes the evaluation of (34) rather difficult. However, when $\omega \ll \omega_c$, the phase velocity is approximately constant given as

$$c_a = V_h\sqrt{\frac{n_c}{n_h}} \tag{36}$$

Now we may proceed to evaluate (34) as

$$\begin{aligned}\psi(\mathbf{r},t) &= \frac{1}{2\pi}\frac{q}{R}\frac{r_h^2}{c_a^2}\int_{-\infty}^{\infty}\omega^2\exp\left\{i\omega\left(\frac{R}{c_a}-t\right)\right\}d\omega \\ &= -\frac{q}{R}\frac{r_h^2}{c_a^2}\delta''\left(\frac{R}{c_a}-t\right)\end{aligned} \tag{37}$$

where δ'' is the second derivative of the delta function.Thus the space-time Green's function for EAW is written as

$$G(\mathbf{r},t;\mathbf{r}',t') = -\frac{U(t-t')}{|\mathbf{r}-\mathbf{r}'|}\frac{r_h^2}{c_a^2}\delta''\left(\frac{R}{c_a}-t\right) \tag{38}$$

where U is the Heaviside unit step-function. Note that this form of Green's function for the EAW is valid only under the approximation that the phase velocity is a constant. As seen in Figure 2 the phase velocity is indeed a constant when $\omega \ll \omega_c$. Therefore, if the signal bandwidth falls well below ω_c the above Green's function is accurate.

3.4 Kinetic Approach to Electron Acoustic Waves

Our study of EAW in the last section was based on a hydrodynamic description of plasma. Although the dispersion relation is correct it does not account for the phenomenon of resonant damping[4] which has a major impact on the ability of EAW to carry low-frequency microwave signals. To assess this impact we adopt a kinetic approach. The fundamental quantity here is the velocity distribution function which is governed by the following equation.

$$\partial_t f + \mathbf{v}\cdot\nabla f = \tfrac{e}{m}\mathbf{E}\cdot\nabla_v f \tag{39}$$

We have one such Vlasov equation for the hot and cold electron populations. Because of its slow velocity, ion population does not play any role in the estimate of resonant damping. We ignore collisions and use a linearized Vlasov equation along with the Poisson equation. Thus we arrive at the following dispersion equation

$$1+\tfrac{1}{k^2r_c^2}\left\{1+\zeta_c Z(\zeta_c)\right\}+\tfrac{1}{k^2r_c^2}\left\{1+\zeta_c Z(\zeta_c)\right\}=0 \tag{40}$$

where Z is the plasma dispersion function defined as

$$Z(\zeta_c)=\tfrac{1}{\pi}\int\tfrac{e^{-y^2}}{y-\zeta}dy \tag{41}$$

and

$$\zeta_c=\tfrac{\omega}{\sqrt{2}kV_\alpha}\qquad\qquad \alpha=\{c,h\} \tag{42}$$

EAW exist in the regime where the phase velocity lies well within the interval between the thermal speeds of hot and cold electrons. In other words we require that $V_h \ll \omega/k \ll V_c$. This means that we need to keep $\zeta_c \gg 1$ and $\zeta_h \ll 1$. The plasma dispersion function has the following asymptotic expansion for $|\zeta| \gg 1$:

$$Z(\zeta)\approx i\sqrt{\pi}\sigma e^{-\zeta^2}-\tfrac{1}{\zeta}\left\{1+\tfrac{1}{2\zeta^2}+\tfrac{3}{4\zeta^4}+\tfrac{15}{8\zeta^6}+\cdots\right\} \tag{43}$$

where

$$\sigma\begin{cases}0 & \zeta''>\frac{1}{|\zeta'|}\\ 1 & \zeta''<\frac{1}{|\zeta'|}\\ 2 & \zeta''<-\frac{1}{|\zeta'|}\end{cases} \tag{44}$$

with $\zeta=\zeta'+i\zeta''$. In the other limiting case when $|\zeta| \ll 1$ we use the following power series representation for Z:

$$Z(\zeta)=i\sqrt{\pi}\sigma e^{-\zeta^2}-2\zeta\left\{1-\tfrac{2\zeta^2}{3}+\tfrac{4\zeta^4}{15}-\tfrac{8\zeta^6}{105}+\cdots\right\} \tag{45}$$

On making use of these representations in (40) and equating the real parts we have

[4] Resonant damping occurs in our problem due to the energy exchange between the electron acoustic wave and particles in the plasma [T.H. Stix, {\it Waves in Plasma}, Springer-Verlag, New York, 1992]. Those particles having velocities less than the phase velocity of the EAW will be accelerated by the EAW. As commonly done, particle velocities are modeled as a Maxwellian distribution function. Thus there are more particles with velocities less than the wave phase velocity. Consequently, there are more particles gaining energy from the wave, and this is the reason for plasma waves to be damped.

$$1-\frac{1}{k^2r_c^2}\mathrm{Re}\left(\frac{1}{2\zeta_c^2}\right)+\frac{1}{k^2r_h^2}\left\{1-\sqrt{\pi}\,\mathrm{Im}(\zeta_h)\right\}=0 \tag{46}$$

Assuming the frequency to be complex by letting $\omega=\omega'+i\omega''$, and imposing the condition that $|\omega''|\ll\omega'$, we obtain the following solution

$$\omega'=\left(\frac{\omega_c^2}{1+k^{-2}r_h^{-2}}\right)^{\frac{1}{2}} \tag{47}$$

which is identical to the result that we obtained using the hydrodynamic approach. We follow a similar procedure by equating the imaginary parts of (40) and obtain the following expression for damping rate:

$$\frac{\omega''}{\omega'}=-\frac{1}{2}\sqrt{\frac{\pi}{2}}\frac{n_c}{n_h} \tag{48}$$

We thus infer that the ratio n_c/n_h has to be very small in order to keep the damping rate acceptable. However, it is impractical to realize this, for example, in reentry applications. Therefore, to maintain an acceptable level of EAW energy we introduce an electron beam into the system. The density of the beam electrons can be small. However its velocity has to resonate with the phase velocity of EAW. With the addition of such an electron beam the dispersion equation now becomes

$$1+\frac{1}{k^2r_c^2}\left\{1+\zeta_cZ(\zeta_c)\right\}+\frac{1}{k^2r_h^2}\left\{1+\zeta_hZ(\zeta_h)\right\}+\frac{1}{k^2r_b^2}\left\{1+\tilde{\zeta}_bZ(\tilde{\zeta}_b)\right\}=0 \tag{49}$$

where

$$\zeta_b=\frac{\omega}{\sqrt{2}kV_b} \tag{50}$$

$$\tilde{\zeta}_b=\zeta_b-\frac{1}{\sqrt{2}}\frac{V_{0b}}{V_b}\cos\theta \tag{51}$$

V_{0b} is the beam velocity and θ is the orientation angle of the beam with respect to the plasma sheath. r_b, and V_b are respectively the Debye radius and thermal speed of the beam electrons. We keep the magnitude of $\tilde{\zeta}_b$ between that of the hot and cold electrons. It is not possible to obtain a closed-form solution to the above dispersion equation. However, one can get an estimate of the damping characteristics by assuming that $|\zeta_b|>1$ and using the asymptotic expansion. Since n_b/n_c is small we find that there is no significant change in the real part of the frequency. However, the imaginary part of the frequency is different and is given as

$$\frac{\omega''}{\omega'}=-\sqrt{\frac{\pi}{2}}\frac{n_c}{n_h}\left\{2+\frac{r_h^2}{r_b^2}\frac{1}{\tilde{\zeta}_b'^2}\frac{\zeta_b'}{\tilde{\zeta}_b'}\right\}^{-1} \tag{52}$$

Notice that since $\tilde{\zeta}_b'$ is much smaller than ζ_b' the attenuation in the scheme with an electron beam is significantly less than without it.

Indeed these estimates are based on asymptotic relations. In general one needs to solve the dispersion equation numerically to identify the regime which is most suitable for the application at hand. Below we present two examples to illustrate the dispersion characteristics of EAW. In the first example we choose the following set of parameters: $n_o=10^{11}\mathrm{cc}^{-1}$, $n_c=0.6n_o$, $n_h=0.4n_o$,

$T_c = 1$ eV, and $T_h = 20$ eV. The results obtained by a numerical solution of (49) are shown in Figure 4.

The complex roots of the dispersion relation, viz., the real and imaginary parts of the frequency, correspond to the real frequency obtained by our hydrodynamic approach and to the wave attenuation due to resonant damping. In Figure 4 we have shown the normalized (normalized with respect to cold electron plasma frequency) frequency and attenuation. Note that the propagation constant is normalized using the Debye radius of the hot electrons. As predicted by our analysis, the damping is very high even though we have chosen the parameters favorable to the existence of EAW. In order to maintain an acceptable level of EAW we have introduced into the system an electron beam whose velocity resonates with the phase velocity of EAW. To illustrate the significance of the electron beam we have chosen an example with the following parameters: $n_o = 10^{11}\text{cc}^{-1}$, $n_c = 0.9n_o$, $n_h = 0.01n_o$, $n_b = 0.09n_o$, $T_c = 1$ eV, $T_h = 20$ eV, $T_b = 0.1$ eV, $V_b = 6.5\times10^8$ cm/s. The solution to the dispersion equation with these set of parameters is shown in Figure 5. Note that total electron density here is the same as in Figure 4. Yet the damping in this case is significantly less than in the case without the beam. Since our interest is in the regime when the operating frequency is much less than the cold plasma frequency, i.e. when the normalized frequency ratio is very small, we see that the damping is fairly small here.

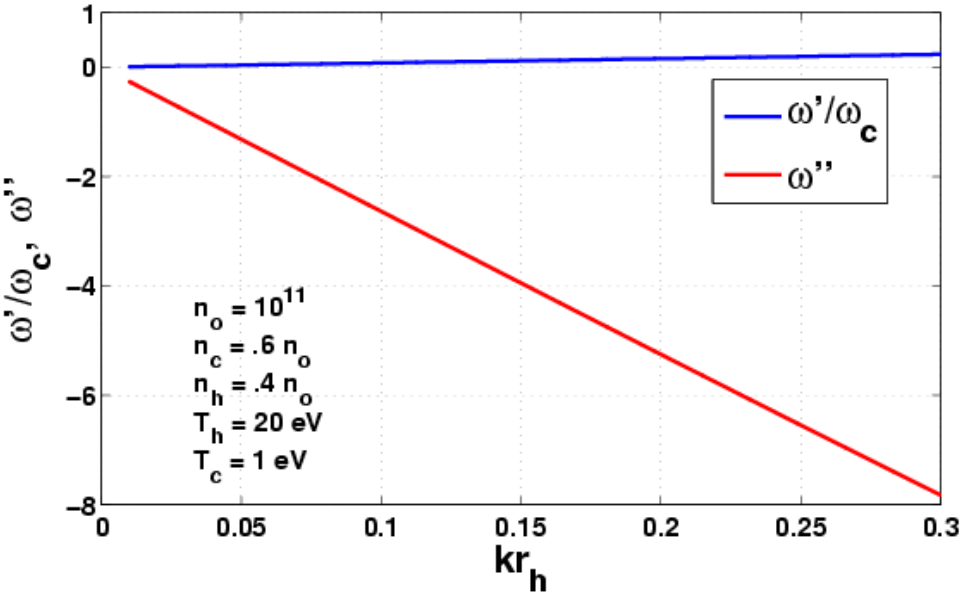

Figure 4. Resonant Damping of Electron Acoustic Waves.

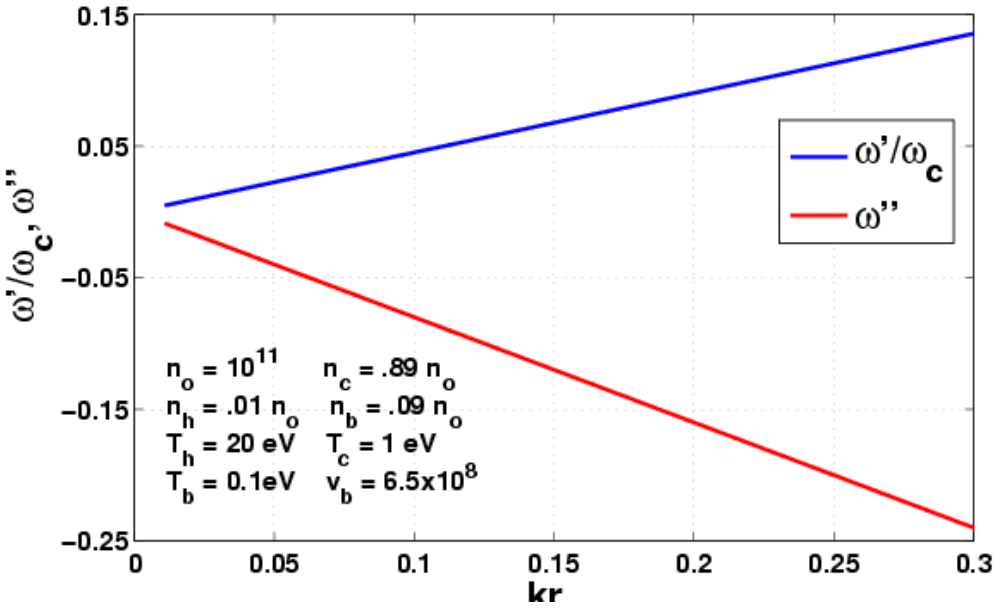

Figure 5. Resonant Damping of Electron Acoustic Waves in the Presence of an Electron Beam.

3.5 Current Sources in the Two-Temperature Electron Population

We are interested in studying the radiation characteristics of a source distribution embedded in an overdense plasma sheath. If it is sufficiently thick (much larger than the skin depth) there will not be any radiation outside the plasma sheath. By injecting into it a small population of hot electrons we create a composite medium made of a two-temperature electron population. The embedded antenna can excite EAW which will then transform into EMW at the boundary of the sheath and hence radiate. The geometry of our problem is shown in Figure 6. The lower half-space is composed of the two-temperature electron population. Embedded in this medium we may have a distribution of current sources. We are interested in the radiation characteristics of these current sources in free space (upper half-space) outside the plasma medium. To facilitate this study we derive the Green's functions for the problem. We denote the lower half-space as Region 1 and the upper half-space as Region 0. Thus $\bar{\mathbf{G}}_{11}$ denotes the Green's function when both the source and observation points are in the lower half-space. We saw that in our two-temperature electron population there can exist two types of waves, viz., EMW and EAW. Hence $\bar{\mathbf{G}}_{11}$ consists of two parts as given below:

$$\bar{\mathbf{G}}_{11} = a\bar{\mathbf{G}}_e + \tilde{\alpha} b \nabla\nabla G_a \tag{53}$$

where the first part represents EMW and the second part represents EAW. More specifically, $\bar{\mathbf{G}}_e$ represents the EMW in our problem and is governed by

$$\nabla\times\nabla\times\bar{\mathbf{G}}_e - k_e^2\bar{\mathbf{G}}_e = \mathbf{I}\delta(\mathbf{r}-\mathbf{r}') \tag{54}$$

G_a represents the EAW for our problem and is governed by

$$\nabla\times\nabla\times G_a - k_a^2 G_a = -\delta(\mathbf{r}-\mathbf{r}') \tag{55}$$

The constants a and b in (53) are given as

$$a = \frac{4\pi i\omega}{c^2} \qquad b = \frac{4\pi i}{\omega|\varepsilon_p|} \tag{56}$$

where

$$\varepsilon_p = 1 - \frac{\omega_p^2}{\omega^2} \tag{57}$$

$\tilde{\alpha}$ is a constant that will be determined on imposing the boundary conditions. The propagation constants k_e (for EMW) and k_a (for EAW) are given as

$$k_e = k_o\left(1-\frac{\omega_p^2}{\omega^2}\right)^{\frac{1}{2}} \qquad k_a = \frac{1}{r_h}\frac{\omega}{\sqrt{\omega_c^2-\omega^2}} \tag{58}$$

The solution for our problem in the case when the source is in the lower half-space and the observation point in the upper half-space is represented by the Green's function $\bar{\mathbf{G}}_{01}$. Noting that the upper half-space supports only EMW the governing equation is given as

$$\nabla\times\nabla\times\bar{\mathbf{G}}_{01} - k_o^2\bar{\mathbf{G}}_{01} = 0 \tag{59}$$

where $k_o = \omega/c$. The boundary conditions associated with these Green's functions are based on the following requirements. The tangential components of the electric and magnetic fields must be continuous across the interface $z = 0$, and the normal components of the velocity vectors of the cold and hot electrons must vanish at the interface. This second condition ensures that the charge distributions of the two-temperature electron population do not drift away and are confined to the geometrical bounds of the plasma sheath. These requirements lead to the following conditions on our Green's functions

$$\hat{z} \times \nabla \times \bar{\mathbf{G}}_{01}(\mathbf{r}_\perp, 0; \mathbf{r}') = \hat{z} \times \nabla \times \bar{\mathbf{G}}_{11}(\mathbf{r}_\perp, 0; \mathbf{r}') \tag{60}$$

$$\hat{z} \times \bar{\mathbf{G}}_{01}(\mathbf{r}_\perp, 0; \mathbf{r}') = \hat{z} \times \bar{\mathbf{G}}_{11}(\mathbf{r}_\perp, 0; \mathbf{r}') \tag{61}$$

$$\tilde{\alpha} R_d^2 \partial_z \nabla^2 \nabla G_a(\mathbf{r}_\perp, 0; \mathbf{r}') = \tilde{\alpha} \partial_z \nabla G_a(\mathbf{r}_\perp, 0; \mathbf{r}') + k_p^2 \hat{z} \cdot \bar{\mathbf{G}}_e(\mathbf{r}_\perp, 0; \mathbf{r}') \tag{62}$$

where $k_p^2 = |k_e|^2$ and R_d is the composite Debye radius defined as

$$R_d = \frac{r_c r_h}{\sqrt{r_c^2 + r_d^2}} \tag{63}$$

where r_c and r_d are the Debye radii of the cold and hot electron populations.

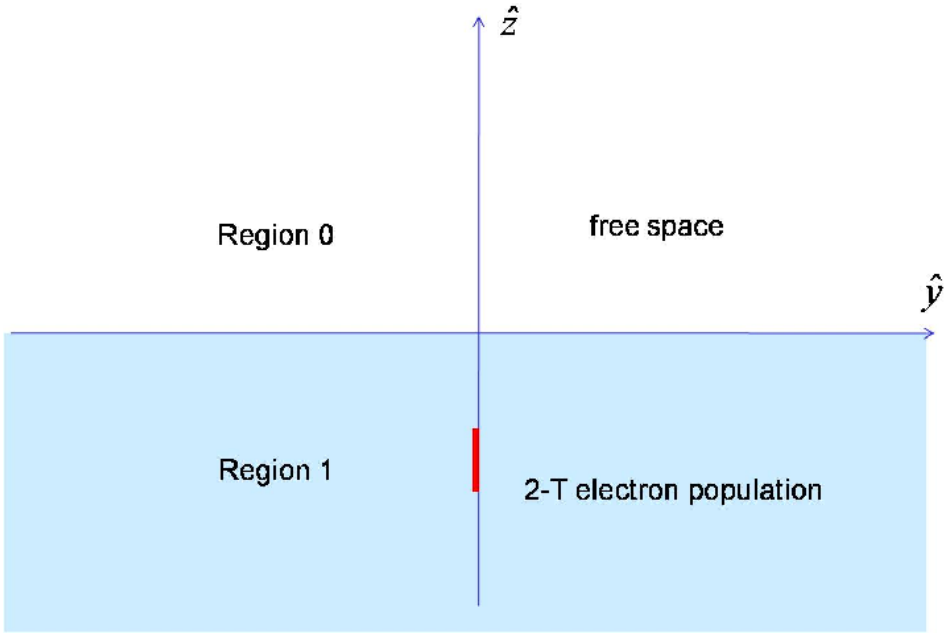

Figure 6. Geometry of the Radiation Problem. The antenna is located on the z-axis

3.6 Formulation of Green's Functions

First we construct the Green's function $\bar{\mathbf{G}}_{11}$ as shown in (51). As given there, it is composed of $\bar{\mathbf{G}}_e$ and G_a as defined in (54) and (55). The solutions for $\bar{\mathbf{G}}_e$ and G_a can be readily written for our geometry. We use the following spectral representations:

$$\bar{\mathbf{G}}_e^{>}(\mathbf{r},\mathbf{r}') = \tfrac{1}{8\pi^2}\int d\mathbf{k}_\perp \tfrac{1}{\eta}\left\{\left(\mathbf{h}^+ e^{i\mathbf{k}_e^+\cdot\mathbf{r}} + R\mathbf{h}^- e^{i\mathbf{k}_e^-\cdot\mathbf{r}}\right)\mathbf{h}^+ + \left(\mathbf{v}^+ e^{i\mathbf{k}_e^+\cdot\mathbf{r}} + S\mathbf{v}^- e^{i\mathbf{k}_e^-\cdot\mathbf{r}}\right)\mathbf{v}^+\right\} e^{-i\mathbf{k}_e^+\cdot\mathbf{r}'} \tag{64}$$

$$G_a^{>}(\mathbf{r},\mathbf{r}') = \tfrac{1}{8\pi^2}\int d\mathbf{k}_\perp \tfrac{i}{q_a}\left\{e^{i\mathbf{k}_a^+\cdot\mathbf{r}} + Se^{i\mathbf{k}_a^-\cdot\mathbf{r}}\right\} e^{-i\mathbf{k}_a^+\cdot\mathbf{r}'} \tag{65}$$

where $\mathbf{h}$ and $\mathbf{v}$ are unit vectors representing horizontal and vertical polarizations of EMW. The superscripts $+$ and $-$ indicate whether the corresponding wave is propagating upwards or downwards. R and S are the reflection coefficients of horizontally- and vertically-polarized waves, respectively, from the interface $z = 0$ when the EM wave is incident from below. $\mathbf{k}_e$ is the wave number vector of the electromagnetic waves, defined as

$$\mathbf{k}_e^{\pm} = \mathbf{k}_\perp \pm \hat{z}i\eta \qquad \eta = \sqrt{k_p^2 + \mathbf{k}_\perp^2} \tag{66}$$

Notice that η is positive and hence the $\hat{z}$ component of $\mathbf{k}_\mathbf{e}$ is imaginary. Thus the EMW in the lower half-space are evanescent in our frequency regime (overdense case). In contrast, the wave number vector of the EAW is given as

$$\mathbf{k}_a^{\pm} = \mathbf{k}_\perp \pm \hat{z}q_a \qquad q_a = \sqrt{k_a^2 - \mathbf{k}_\perp^2} \tag{67}$$

where the $\hat{z}$ component of the wave number vector is real and hence corresponds to propagating waves. The superscript $>$ on $\bar{\mathbf{G}}_e$ and G_a indicates that the representations are for the case when $z > z'$. The corresponding representations for the case when $z < z'$ may be obtained using the following symmetry relations:

$$\bar{\mathbf{G}}_e^{>}(\mathbf{r},\mathbf{r}') = \bar{\mathbf{G}}_e^{<t}(\mathbf{r}',\mathbf{r}) \tag{68}$$

$$G_a^{>}(\mathbf{r},\mathbf{r}') = G_a^{<}(\mathbf{r}',\mathbf{r}) \tag{69}$$

where the superscript t denotes transpose. Using these Green's functions we may construct $\bar{\mathbf{G}}_{11}^{>}$ and $\bar{\mathbf{G}}_{11}^{<}$. However, notice that we only need $\bar{\mathbf{G}}_{11}^{>}$ for imposing the boundary conditions at the $z = 0$ interface. We construct $\bar{\mathbf{G}}_{01}$ noting that only EMW can exist in the upper half-space. Thus the spectral representation for $\bar{\mathbf{G}}_{01}$ is given as

$$\bar{\mathbf{G}}_{01}(\mathbf{r},\mathbf{r}') = \tfrac{1}{8\pi^2}\int d\mathbf{k}_\perp e^{-i\mathbf{k}_o^+\cdot\mathbf{r}}\left\{\tfrac{a}{\eta}\left(X\mathbf{h}_o^+\mathbf{h}^+ + Y\mathbf{v}_o^+\mathbf{v}^+\right)e^{-i\mathbf{k}_e^+\cdot\mathbf{r}'} + \tilde{\alpha}Yb\tfrac{i}{q_a}\mathbf{v}_o^+\left(\mathbf{k}_a^+ + S\mathbf{k}_a^-\right)e^{-i\mathbf{k}_a^+\cdot\mathbf{r}'}\right\} \tag{70}$$

The subscript o is used to denote the polarization vectors in the upper half-space. The propagation vector in the upper half-space is defined as

$$\mathbf{k}_o^{\pm} = \mathbf{k}_\perp \pm \hat{z}k_{oz} \qquad k_{oz} = \sqrt{k_o^2 - \mathbf{k}_\perp^2} \tag{71}$$

On substituting the above representations of Green's functions in the boundary conditions one may obtain solutions for the various coefficients. Instead of trying solve this general boundary value problem it is much easy to obtain the solution that corresponds to a specific source current configuration.

4. Results and Discussion

4.1 Radiation Pattern of a Hertzian Dipole

With the availability of the Green's functions we may calculate the radiation characteristics of any source current distribution in our composite medium. Since we are interested in the far-field radiation pattern in the upper half-space we need the asymptotic form of $\bar{\mathbf{G}}_{01}(\mathbf{r},\mathbf{r}')$ when $kr \gg 1$. Evaluating (70) using the method of steepest descent we obtain the following asymptotic result:

$$\bar{\mathbf{G}}_{01}(\mathbf{r},\mathbf{r}') \sim -k_o k_{oz} \frac{1}{c}\frac{e^{ik_o r}}{r}\left\{\frac{1}{\eta}\left(X\mathbf{h}_o^+\mathbf{h}^+ + Y\mathbf{v}_o^+\mathbf{v}^+\mathbf{h}^-\right)e^{-i\mathbf{k}_e^+\cdot\mathbf{r}'} - \frac{\tilde{\alpha}}{k_p^2}\frac{i}{q_a}Y\mathbf{v}_o^+\left(\mathbf{k}_a^+ + S\mathbf{k}_a^-\right)e^{-i\mathbf{k}_a^+\cdot\mathbf{r}'}\right\} \tag{72}$$

Note that all quantities in the above expression are evaluated at θ, which is the elevation angle associated with the observation point $\mathbf{r}$. Using this representation of the Green's function we can calculate the far-zone radiating fields corresponding to arbitrary source current distributions embedded in our composite medium. Suppose $\mathbf{J}$ is the source current distribution in our composite medium. Its far-zone radiation fields in the upper half-space are given as

$$\mathbf{E}(\mathbf{r}) = \int_{-\infty}^{0} \bar{\mathbf{G}}_{01}(\mathbf{r},\mathbf{r}')\cdot\mathbf{J}(\mathbf{r}')d\mathbf{r}' \tag{73}$$

On substituting (72) in (53) we obtain the following expressions for θ and ϕ components of the electric fields:

$$\left|E_\phi(\mathbf{r})\right| \sim k_o k_{oz}\frac{1}{cr}\left|X\right|\left|\int \mathbf{h}^+\cdot\mathbf{J}(\mathbf{r}')e^{-i\mathbf{k}_\perp\cdot\mathbf{r}'}e^{\eta z'}d\mathbf{r}'\right| \tag{74}$$

$$\left|E_\theta(\mathbf{r})\right| \sim k_o k_{oz}\frac{1}{cr}\frac{\tilde{\alpha}}{q_a k_p^2}\left|Y\right|\left|\int\left(\mathbf{k}_a^+ + S\mathbf{k}_a^-\right)\cdot\mathbf{J}(\mathbf{r}')e^{-i\mathbf{k}_\perp\cdot\mathbf{r}'}e^{-iq_a z'}d\mathbf{r}'\right| \tag{75}$$

For sources not too close to the interface we hence notice that $\left|E_\phi(\mathbf{r})\right|$ is exponentially small. Indeed, if the sources are very close to the interface the radiation will not be affected much by the overdense plasma and hence there is no need to create a two-temperature electron population. It is only in the case when the current sources are well away from the interface in the overdense plasma that we need to inject a hot electron population as suggested in this report to facilitate low-frequency signal transmission across the plasma. Thus, for any source distribution which is not too close to the interface the radiated fields are entirely θ-polarized. In this sense the plasma sheath may hence be regarded as a polarization filter that filters out ϕ-polarized signals.

More detailed characteristics of the radiation pattern may be inferred only when we know about the various coefficients that appear in the Green's functions. As mentioned earlier these coefficients are obtained by imposing the boundary conditions. For an arbitrary source distribution it is fairly complicated to evaluate the coefficients. We hence focus attention on two specific cases.

4.2 Vertical Hertzian Dipole

In this case we choose the source current to be

$$\mathbf{J}(\mathbf{r}) = \hat{z} J_o \delta(\mathbf{r}_\perp)\delta(z+d) \tag{76}$$

where J_o is its amplitude. Substituting this in (74) and (75) we obtain the following solution for the far-zone scattered fields:

$$\mathbf{E}(\mathbf{r}) = -\hat{\theta} k_o k_{oz} \frac{e^{ik_o r}}{cr} \frac{i\tilde{\alpha}_\perp}{k_p^2} Y_\perp \left(1 - S_\perp\right) J_o e^{iq_a d} \tag{77}$$

Further, employing the boundary conditions we obtain the following solutions for the various coefficients:

$$\tilde{\alpha}_\perp = \frac{ik_p^2}{\eta q_a} \frac{\sin^2\theta}{1+k_a^2 R_d^2} \tag{78}$$

$$S_\perp = \frac{k_p \cos\theta - \xi - \nu_p k_p \cos\theta_o}{k_p \cos\theta - \xi + \nu_p k_p \cos\theta_o} \tag{79}$$

$$Y_\perp = \frac{2i\nu_p k_p \sin\theta\left(k_p \cos\theta - \xi\right)}{iD_\perp k_p \sin\theta + 2\tilde{\alpha}\eta\nu_p \cos\theta_o} \tag{80}$$

$$\xi = -i\tilde{\alpha}\eta \qquad \nu_p = \frac{k_p}{k_o} \tag{81}$$

$$D_\perp = k_p \cos\theta - \xi + \nu_p k_p \cos\theta_o \tag{82}$$

Notice that the problem has azimuthal symmetry and hence the above expressions are independent of azimuthal angle. We have used the subscript $\perp$ to indicate that these solutions are for the vertically-polarized Hertzian dipole.

To illustrate the radiation characteristics of the vertical dipole, we have chosen the following numerical example. The electron density is chosen as $10^{12}[\mathrm{cc}^{-1}]$, 5 % of which constitute the hot electron population. The temperatures of the cold and hot electrons are 0.2 eV and 20 eV, respectively. The signal frequency of the antenna is taken as 1 GHz. Since the plasma frequency for this example is around 9 GHz, we are operating in the overdense region and hence we need a scheme like the two-temperature electron population to transmit signals across the plasma sheath. As explained in the report the EAW can carry low-frequency microwave signals across the overdense region. They get transformed into EMW at the plasma free-space interface and hence radiate. As mentioned earlier, the ϕ-polarized components of the electric fields are exponentially small and hence only the θ-polarized components radiate. A polar plot of the radiation pattern is shown in Figure 7. The radiation pattern of the vertical dipole embedded in the plasma is shown in red and that in free space is shown in blue. We see that the radiation is skewed at an oblique angle. This is typical for our problem. The skew angle may change depending on the parameters, but the radiation pattern is always found to be skewed at some angle.

It is of interest to compare the radiated fields for this overdense case with those of an underdense case. When the electron density is sufficiently small such that $\omega_p < \omega$, we have the

underdense situation. The electron density in our example is $10^8[\mathrm{cc}^{-1}]$, which corresponds to the plasma frequency if around 90 MHz. This is the underdense situation. From the dispersion relations (58) we see that k_e now is real and k_a is imaginary. Thus the EAW are now exponentially small and it is now the EMW that carry the microwave signals. The radiated fields are given as

$$\mathbf{E}(\mathbf{r}) = \hat{\theta} k_o \frac{e^{ik_o r}}{cr} \frac{ik_o}{k_p} Y J_o e^{-q_a d} \sin\theta \tag{83}$$

where

$$Y = \frac{2k_p \cos\theta_o}{k_o \cos\theta + k_p \cos\theta_o}$$

$$q = \left\{ k_p^2 - k_o^2 \sin^2\theta \right\}^{\frac{1}{2}} \tag{84}$$

The normalized magnitude of the radiated fields for this case is shown (green) in Figure 7 for comparison.

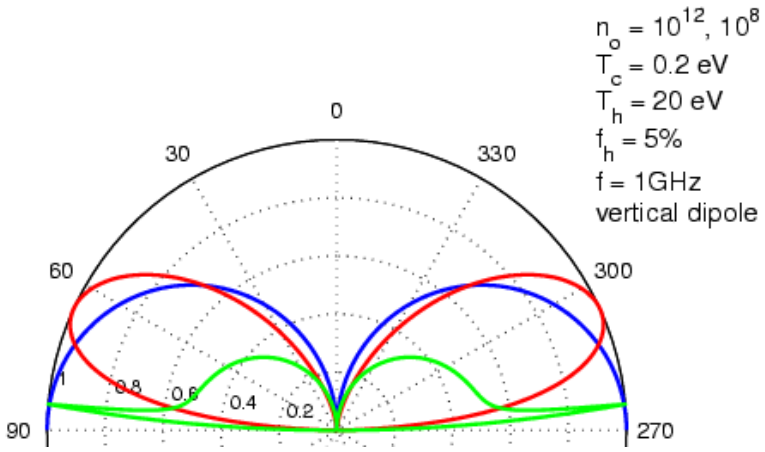

Figure 7. Comparison of radiation patterns of a vertical dipole in plasma.

We next turn our attention to the other important case when the dipole is oriented parallel to the interface.

4.3 Horizontal Hertzian Dipole

We now choose the source to be

$$\mathbf{J}(\mathbf{r}) = \hat{z} J_o \delta(\mathbf{r}_\perp)\delta(z+d) \tag{85}$$

where $\hat{\rho}$ is a unit vector on the horizontal plane (that indicates the orientation of the dipole). Substituting this in (74) and (75) we obtain the following solution for the far-zone radiated fields.

$$\mathbf{E}(\mathbf{r}) = -\hat{\theta} k_o^2 k_{oz} \frac{e^{ik_o r}}{cr} \frac{i\tilde{\alpha}_{\square}}{k_p^2 q_a} Y_{\square} \left(1 + S_{\square}\right) J_o \cos\phi \tag{86}$$

where ϕ is the azimuth angle that the plane of observation makes with the ρ-z plane.
Further, employing the boundary conditions we obtain the following solutions for the various coefficients:

$$R = \frac{k_p \cos\theta - k_o \cos\theta_o}{k_p \cos\theta + k_o \cos\theta_o} \tag{87}$$

$$X = \frac{2k_p \cos\theta}{k_p \cos\theta + k_o \cos\theta_o} \tag{88}$$

$$\tilde{\alpha}_{\square} = \frac{i\sqrt{q_a}\cos\theta}{2\eta\sqrt{\Upsilon}\sin^2\theta}\left\{\sqrt{\Upsilon q_a}\nu_p \cos\theta_o \pm \left(\Upsilon q_a \nu_p^2 \cos^2\theta_o + 4k_p \sin^2\theta\cos\theta\right)^{\frac{1}{2}}\right\} \tag{89}$$

$$S_{\square} = \frac{iq_a \cos\theta\left(\cos\theta - \nu_p \cos\theta_o\right) + \tilde{\alpha}\eta\sin^2\theta}{iq_a \cos\theta\left(\cos\theta + \nu_p \cos\theta_o\right) - \tilde{\alpha}\eta\sin^2\theta} \tag{90}$$

$$Y_{\square} = \frac{2i\nu_p k_p^2 \cos^2\theta}{D_{\square} k_p^2 - 2\alpha\eta k_o \cos\theta\cos\theta_o} \tag{91}$$

$$D_{\square} = iq_a \cos\theta\left(\cos\theta + \nu_p \cos\theta_o\right) - \tilde{\alpha}\eta\sin^2\theta \tag{92}$$

$$\Upsilon = 1 + k_a^2 R_d^2 \tag{93}$$

The subscript $\square$ is used to indicate that these solutions correspond to the case of the horizontal dipole. Notice that in this case there are two solutions for $\tilde{\alpha}_{\square}$. For the parameters of our problem it turns out that the solution with the positive value of the discriminant is nonphysical. Hence we take the value for $\tilde{\alpha}_{\square}$ with the negative discriminant as the solution. As before, the ϕ-components of the electric fields are exponentially small; only their θ-components are radiated. Figure 8 shows the radiation pattern in the vertical plane parallel to the dipole. As before, the radiation pattern for the horizontally-oriented dipole embedded in the overdense plasma is shown in red. The corresponding results for the dipole in free space are shown in blue. Actually the blue curve is not visible because it is overshadowed by the green curve that represents the underdense case. For illustration, we have chosen the same parameters as for the vertical dipole. We see that there is a significant skew towards $\theta = 90^\circ$. More importantly there is a complete absence of radiation in the broad-side region. In other words, the radiation is close to the end-fire direction. Thus this configuration is not suitable for constructing phased arrays intended for beam sweeping around the broad side.

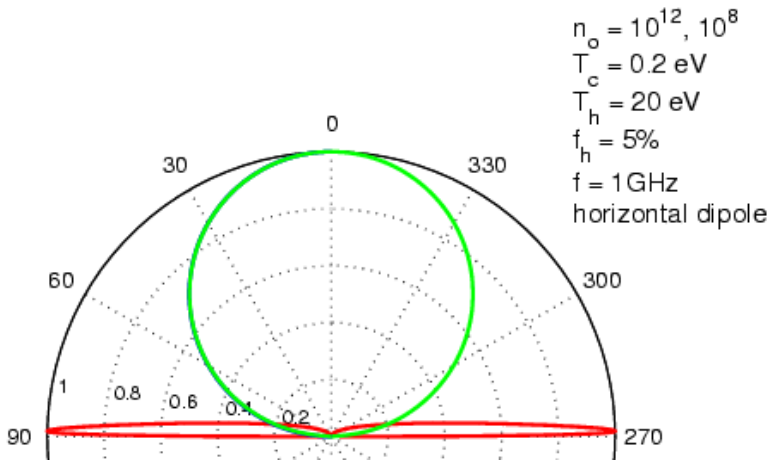

Figure 8. Comparison of radiation pattern of horizontal dipole in plasma.

We now look at the underdense case for the horizontal dipole. Again the EAW are exponentially small and hence our microwave signals are carried entirely by EMW. The radiated field in this case is given as

$$\mathbf{E}(\mathbf{r}) = k_o k_{oz} \frac{e^{ik_o r}}{cr} \frac{i}{k_z} e^{-ik_z d} J_o \left\{ -\hat{\theta} Y \cos\theta \cos\phi + \hat{\phi} X \sin\phi \right\} \tag{94}$$

where X and Y are given earlier. As expected, the radiated fields contain both θ- and ϕ-polarized waves. The normalized amplitude of the electric fields in the ρ-z plane is shown (green) in Figure 8 for comparison. Note that the result coincides with the normalized amplitude of the electric field for the dipole in free-space.

In the next section we turn our attention to the radiation characteristics of an arbitrarily-oriented Hertzian dipole.

4.4 Hertzian Dipole with Arbitrary Orientation

The source current of the Hertzian dipole with arbitrary orientation is represented as

$$\mathbf{J}(\mathbf{r}) = \left(\hat{\rho} J_{\rho} + \hat{z} J_{z}\right)\delta(\mathbf{r}_{\perp})\delta(z+d) \tag{95}$$

where J_{ρ} and J_{z} are the components of the source current. As before, the amplitude of this current is J_{o} and its direction is denoted by the unit vector $\hat{J}$. Using the results for the horizontally- and vertically-oriented dipoles we may construct the Green's function for our problem as

$$\bar{\mathbf{G}}_{01}(\mathbf{r},\mathbf{r}') = \bar{\mathbf{G}}_{\perp} \cdot \hat{z}\hat{z} + \bar{\mathbf{G}}_{\square} \cdot \hat{\rho}\hat{\rho} \tag{96}$$

where

$$\bar{\mathbf{G}}_{p}(\mathbf{r},\mathbf{r}') = \frac{1}{8\pi^2}\int d\mathbf{k}_{\perp} e^{-i\mathbf{k}_{o}^{+}\cdot\mathbf{r}} \left\{ \frac{a}{\eta}\left(X_{p}\mathbf{h}_{o}^{+}\mathbf{h}^{+} + Y_{p}\mathbf{v}_{o}^{+}\mathbf{v}^{+}\right) e^{-i\mathbf{k}_{e}^{+}\cdot\mathbf{r}'} + \tilde{\alpha} Y_{p} \frac{ib}{q_{a}} \mathbf{v}_{o}^{+}\left(\mathbf{k}_{a}^{+} + S_{p}\mathbf{k}_{a}^{-}\right) e^{-i\mathbf{k}_{a}^{+}\cdot\mathbf{r}'} \right\} \tag{97}$$

and $p = \{\perp, \square\}$. Thus the far-zone radiated field from an arbitrarily-oriented Hertzian dipole located at $z = -d$ is given as

$$\mathbf{E}(\mathbf{r}) = \bar{\mathbf{G}}_{01}(\mathbf{r};0,-d)\cdot\mathbf{J} \tag{98}$$

Thus we can calculate the radiation characteristics of an arbitrary source distribution embedded in the overdense plasma.

We hence see that a two-temperature electron population may be used to transmit low-frequency signals across an overdense plasma. However, there are peculiarities and limitations. We found that only θ-polarized waves are radiated. Further the radiation is skewed towards large θ values. This is not a major set-back for the vertically-oriented dipole. However, the horizontally-oriented dipole has serious limitations in its ability to be used in phased arrays intended for scanning in the broadside.

5. Conclusion

We have studied in this report the radiation characteristics of a source distribution in an overdense plasma composed of a two-temperature population. Indeed, low-frequency EM signals will be completely cut off in this case and hence will not be able to radiate. However, the two-temperature electron population supports EAW whose dispersion relation complements that of the EMW in the sense that EAW propagate in the frequency domain where EMW are cut off and vice versa. Thus in principle one may employ EAW to carry low-frequency microwave signals across an overdense plasma. Unfortunately resonant damping can seriously limit this scheme. However, we find that with the introduction of an electron beam into the system it is possible to keep the damping rate to an acceptable level for our application[5].

We have ignored collisions in our analysis primarily to focus on the concepts of EAW without the complexities associated with the inclusion of collisions. We admit that there will be collisions within the plasma sheath. However, we find that in the domain of our interest the collision frequency is much smaller than the plasma frequency [4]. As with any plasma wave process the electron acoustic waves will undergo certain amount of attenuation because of collisions. However attenuation due to resonant damping is far more significant than that due to collisions. Even in the region of resonant damping our analysis in Section V shows that the real part of frequency of the EAW is unaffected (see eqn (47)). The primary consequence of resonant damping is increased attenuation. Therefore, collisions will not alter the fundamental character of EAW. In particular, the dispersion relation of EAW as shown in Figure 2 will remain unaffected. Our initial study confirms this. Collisions will only introduce additional attenuation of the electron acoustic waves.

To facilitate our study of the radiation characteristics of an arbitrary source distribution embedded in this composite medium we derived the Green's function for our problem. We hence find that only θ-polarized waves can radiate from our system. To understand the characteristics of our system we computed the radiation patterns of vertically- and horizontally-oriented dipoles embedded in our medium. It is found that the radiation pattern of horizontally-polarized waves has two lobes (in contrast to the underdense case) which are strongly skewed towards the horizon. This property makes this configuration unsuitable for constructing phased arrays intended for beam sweeping around the broad side. To summarize, we have found that one can use EAW to transmit low-frequency signals across an overdense plasma. However, there are peculiarities and limitations that one should be aware of before embarking on the design of sensor systems aboard hypersonic vehicles. For instance, we have assumed that we can create a stable two-temperature electron population by injecting a small percentage of hot electrons into the cold electron population that constitutes the overdense hypersonic flow field. The hot electrons may be injected by means of an electron gun on board the hypersonic vehicle like it was done in the CHARGE-2B experiments [28]. However, more theoretical and experimental studies need to be carried out on how to

[5] Indeed there are engineering issues that need to be addressed while implementing the ideas of this scheme in practice

successfully implement this scheme for our application. Another issue concerns the transformation of EAW to EMW. We are aware that this process is not as efficient as we would like it to be. There are limitations on the power of the antennas below which one needs to operate to implement this scheme. Investigation of these issues and finding ways to mitigate them requires further detailed study far beyond the scope of this report. We continue to actively work on these problems details of which will be reported in future publications.

6. References

[1] V. Gorelov, M. Gladyshev, A. Kireev, A. Korolev, I. Yegorov, and V. Byzov, "Compuational and experimental investigations of ionization near hypersonic vehicles," *J. Spacecraft Rockets*, vol. 33, pp. 800–806, 1996.

[2] D. Hall, C. Dougherty, D. Hudson, and N. Rajendran, Reentry Aerothermal Chemistry," Science Applications International Corporation, King of Prussia PA, Tech. Rep. EADD II-31-10543, 2003.

[3] E. Langberg, "Optical communication during hypersonic reentry," *IRE Trans. Commun. Syst.*, vol. 7, pp. 68–70, 1959.

[4] D. Morabito and K. T. Edquist, "Communications blackout predictions for atmospheric reentry of Mars Science Laboratory," in *Proceedings- 2005 IEEE Aerospace Conference*. New Jersey: IEEE Computer Society, 2005.

[5] R. Rawhouser, "Methods of improving radio-wave propagation through the plasma sheath," in *Propagation Factors in Space Communications*. Maidenhead, England: Technivision, 1967, pp. 327–36.

[6] M. P. Bachinski, "Electromagnetic wave penetration of reentry plasma sheaths," *J. Res. NBS*, vol. 69D, pp. 145–154, 1965.

[7] ——, "Radio-wave propagation through re-entry plasma sheaths," in *Propagation Factors in Space Communications*. England: Technivision Maidenhead, 1967, pp. 287–308.

[8] H. Hodara, "The use of magnetic fields in the elimination of the re-entry radio blackout," *Proc IRE*, vol. 49, pp. 1825–1830, 1961.

[9] G. Rosen, "Method for removal of free electrons in plasma," *Phys. Fluids*, vol. 5, pp. 737–737, 1962.

[10] G. G. Cloutier and A. I. Carswell, "Plasma quenching by electro-negative gas seeding," *Phys. Rev. Letters*, vol. 10, pp. 327–327, 1963.

[11] R. Betchov and E. A. Fuhs, "Modification of the electrical properties of the plasma sheath by contaminant injection," in *Electromagnetic Aspects of Hypersonic Flight*, W. Rotman, H. K. Moore, and R. J. Papa, Eds. Baltimore: Spartan, 1964, pp. 1–11.

[12] R. J. Papa and R. L. Taylor, "High-pwer electromagnetic transmission characteristics of a diffusing reentry plasma," *J. Appl. Phys.*, vol. 45, pp. 694–696, 1974.

[13] D. T. Hayes, S. B. Herskovitz, J. F. Lenon, and J. L. Poirier, "Electrostatic probe measurements of chemical injection effects during re-entry flight test," *J. Spacecraft Rockets*, vol. 11, pp. 388–400, 1974.

[14] J. P. Rybak and R. J. Churchill, "Progress in reentry communications," *IEEE Trans Aerospace and Electronic Systems*, vol. 5, pp. 879–894, 1971.

[15] S. V. Nazarenko, A. C. Newell, and V. E. Zakharov, "Communications through plasma sheaths via Raman (three-wave) scattering process," *Phys. Plasmas*, vol. 1, pp. 2827–2834, 1994.

[16] S. V. Nazarenko, A. C. Newell, and A. M. Rubenchik, "Communications with reentry space vehicles via short pulses," *Radio Sci.*, vol. 30, pp. 1753–1766, 1995.

[17] M. Keidar, M. Kim, and I. D. Boyd, "Electromagnetic reduction of plasma density during atmospheric reentry and hypersonic flights," *J. Spacecraft Rockets*, vol. 45, pp. 445–453, 2008.

[18] M. Kim, M. Keidar, and I. D. Boyd, "Analysis of an electromagnetic mitigation scheme for reentry telemetry through plasma," *J. Spacecraft Rockets*, vol. 45, pp. 1223–1229, 2008.

[19] ——, “Two-dimensional model of an electromagnetic layer for the mitigation of communication blackout,” *AIAA paper*, pp. 1232–1232, 2009.
[20] N. Sternberg and A. Smolyakov, “Resonant transmission of electromagnetic waves in multilayer dense-plasma structures,” *IEEE Trans. Plasma Science*, vol. 37, pp. 1251–1260, 2009.
[21] ——, “Resonant transparency of a three-layer structure containing the dense plasma region,” *Progress in Electromagnetic Research*, vol. 99, pp. 37–52, 2009.
[22] I. F. Belov, V. Y. Borovoy, V. A. Gorelov, A. Y. Kireev, A. S. Korolev, and E. A. Stepanov, “Investigation of remote antenna assembly for radio communication with reentry vehicle,” *J. Spacecraft and Rockets*, vol. 33, pp. 800–806, 2001.
[23] R. P. Starkey, “Nonequilibrium plasma effects on telemetry considerations for air-breathing vehicle design,” in *42nd AIAA Aerospace Sciences Meeting and Exhibit*. AIAA, 2004, pp. 3185–3194.
[24] M. Wolverton, “Piercing the plasma : ideas to beat the communications blackout of reentry,” *Scientific American*, December 2009.
[25] G. Norris, “Best concepts for penetrating plasma in future Mach 10+ vehicles,” *Aviation Week and Space technology*, vol. 30, pp. 58–58, March 2009.
[26] V. I. Sotnikov, D. Rose, and S. Mudaliar, “Communication scheme for a two-electron-temperature plasma sheath,” 2010, to be submitted for publication in Physics of Plasmas.
[27] V. I. Sotnikov, D. Schriver, M. Asour-Abdalla, and J. Ernstmeyer, “Excitation of sideband emissions by a modulated electron beam during the CHARGE 2B mission,” *J. Geophys. Res.*, vol. 99 No. A5, pp. 8917–8923, 1994.
[28] V. I. Sotnikov, D. Schriver, M. Asour-Abdalla, J. Ernstmeyer, and N. Meyers, “Excitation of electron acoustic waves by a gyrating electron beam,” *J. Geophys. Res.*, vol. 100, pp. 19 765–19 772, 1995.
[29] D. Schriver, V. I. Sotnikov, M. Asour-Abdalla, and J. Ernstmeyer, “Propagation of beam-driven VLF waves from the ionosphere toward ground,” *J. Geophys. Res.*, vol. 100, pp. 3693–3702, 1995.
[30] D. Schriver, M. Asour-Abdalla, V. I. Sotnikov, P. Hellinger, and A. Mangeney, “Excitation of electron acoustic waves near the electron plasma frequency and at twice the plasma frequency,” *J. Geophys. Res.*, vol. 105, pp. 12 919–12 927, 2000.
[31] E. Marsch, “Beam-driven electron acoustic waves upstream of the earth’s bow shock,” *J. Geophys. Res.*, vol. 90, pp. 6327–6336, 1985.
[32] M. F. Thomsen, H. Barr, S. P. Gary, W. C. Feldman, and T. E. Cole, “Stability of electron distribution with the earth’s bow shock,” *J. Geophys. Res.*, vol. 88, pp. 3035–3045, 1983.
[33] S. Matsukiyo, R. A. Treuman, and M. Scholer, “Coherence in auroral upward current,” *J. Geophys. Res.*, vol. 109, pp. 1–5, 2004.
[34] B. B. Kadomtsev and O. P. Pogutse, “Trapped particles in torroidal magnetic systems,” *Nuclear Fusion*, vol. 11, pp. 67–92, 1971.
[35] W. C. Feldman, J. K. Asbridge, S. J. Bame, M. D. Montgomery, and S. P. Gary, “Solar wind electrons,” *J. Geophys. Res.*, vol. 80, pp. 4181–4196, 1975.
[36] W. C. Feldman, R. C. Anderson, S. J. Bame, J. T. Gosling, R. D. Zwicki, and E. J. Smith, “Electron velocity distribution near interplanetary shocks,” *J. Geophys. Res.*, vol. 88, pp. 9949–9958, 1983.

[37] F. Valentini, T. M. O'Neil, and D. H. E. Dublin, "Excitation of nonlinear electron acoustic waves," *Phys. Plasmas*, vol. 13, no. 052303, 2006.
[38] F. Anderegg, C. Driscoll, D. H. E. Dublin, T. M. O'Neil, and F. Valentini, "Electron acoustic waves in pure ion plasmas," *Phys. Plasmas*, vol. 16, no. 055705, 2009.
[39] S. Ikezawa and Y. Nakamura, "Electron plasma waves in a two-temperature plasma," *J. Phys. Soc. Japan*, vol. 48, pp. 2091–2097, 1980.
[40] ——, "Observation of electron plasma waves in two-temperature electrons," *J. Phys. Soc. Japan*, vol. 50, pp. 962–967, 1981.
[41] S. P. Gary and R. L. Tokar, "The electron-acoustic mode," *Phys. Fluids*, vol. 28, pp. 2439–2441, 1984.

List of Acronyms, Abbreviations, and Symbols

Acronym	Description
EMW	Electromagnetic waves
EAW	Electron Acoustic Waves
E	Electric field
J	Source current
n_o	Electron number density
k_e	Wave number of EMW
k_a	Wave number of EAW
ω_p	Plasma Frequency
Z	Plasma Dispersion Function
r_h, r_c	Debye radii of hot and cold electrons